Supplement of Atmos. Chem. Phys., 21, 18247–18261, 2021
https://doi.org/10.5194/acp-21-18247-2021-supplement

Atmospheric Chemistry and Physics
Open Access
EGU

Supplement of

Modeling secondary organic aerosol formation from volatile chemical products

Elyse A. Pennington et al.

Correspondence to: Havala O. T. Pye (pye.havala@epa.gov)

SAPRC07TIC_AE7I_VCP assignment rules:

Note: Mapping for SOA and radical chemistry are independently treated. Therefore, double mapping may occur. Rules are based on contents of SMILES, k_{OH}, calculated log(C*), number of oxygens (n_O), number of carbons (n_C), and estimated SOA yield.

SOA Chemistry -

1. If SMILES string contains "Si" (i.e. it's a siloxane or silane), add it fully (fraction = 1.0) to **SILOX**.
2. If a species has a SPECIATE_ID = 9001-9032 (i.e. it's new), follow these rules to assign it fully (fraction = 1.0) to one of the new surrogates. IVOP3/4/5/6/5ARO/6ARO definitions are based on Lu et al. (2020). If a species is mapped to IVOC, NVOL, or NROG (US EPA, 2019), follow these rules to re-assign the existing fraction.
    1. If the species has an estimated SOA yield = 0.0%, assign it to **NONR**.
    2. If the species has $n_O > 0$ and an estimated SOA yield > 0.0%, assign it to **SOAOXY**.
    3. If the species has $n_O = 0$, an estimated SOA yield > 0.0%, and has log(C*) > 6.5, assign it to **SOAALK** (both aromatic and aliphatic species).
    4. If the species has $n_O = 0$, an estimated SOA yield > 0.0%, is aromatic, and has 5.5 < log(C*) < 6.5, assign it to **IVOCP6ARO**.
    5. If the species has $n_O = 0$, an estimated SOA yield > 0.0%, is aromatic, and has log(C*) < 5.5, assign it to **IVOCP5ARO**.
    6. If the species has $n_O = 0$, an estimated SOA yield > 0.0%, is aliphatic, and has 5.5 < log(C*) < 6.5, assign it to **IVOCP6**.
    7. If the species has $n_O = 0$, an estimated SOA yield > 0.0%, is aliphatic, and has 4.5 < log(C*) < 5.5, assign it to **IVOCP5**.
    8. If the species has $n_O = 0$, an estimated SOA yield > 0.0%, is aliphatic, and has 3.5 < log(C*) < 4.5, assign it to **IVOCP4**.
    9. If the species has $n_O = 0$, an estimated SOA yield > 0.0%, is aliphatic, and has log(C*) < 3.5, assign it to **IVOCP3**.
3. If an existing species is mapped to ALK4/5 and has an estimated SOA yield > 0.0%, assign it fully (fraction = 1.0) to **SOAALK**.
4. Four species are uniquely treated:
    1. Divinyl Benzene (SPECIATE_ID = 2081): assign fully (fraction = 1.0) to **ARO2MN**.
    2. Styrene (SPECIATE_ID = 698): assign fully (fraction = 1.0) to **ARO2MN**.
    3. Dimethyl Succinate (SPECIATE_ID = 420): assign fully (fraction = 1.0) to **SOAOXY**.
    4. Fragrances (SPECIATE_ID = 467): assign fully (fraction = 1.0) to **IVOCP6** and fully (fraction = 1.0) to **ALK5**.
5. Maintain all other original SAPRC07TC_AE7 assignments.
6. Replace all ARO2 assignments with ARO2MN to match CMAQ's EmissCtrl naming.

Radical Chemistry -

1. If SMILES string contains "Si" (i.e. it's a siloxane or silane), ignore. According to the SAPRC07 database (Carter, 2010), siloxanes have a negative MIR. No applicable surrogate available in SAPRC07.
2. If a species has a SPECIATE_ID = 9001-9032 (i.e. it's new), follow these rules to assign it fully (fraction = 1.0) to ALK1/2/3/4/5. If a species is mapped to IVOC, NVOL, or NROG, follow these rules to re-assign the existing fraction. k_{OH} rules are based on definitions in CMAQ (US EPA Office of Research and Development, 2020).
    a. If 1.35E-13 < k_{OH} < 3.38E-13 cm^3 $molec^{-1}$ sec^{-1}, assign to **ALK1**.
    b. If 3.38E-13 < k_{OH} < 1.69E-12 cm^3 $molec^{-1}$ sec^{-1}, assign to **ALK2**.
    c. If 1.69E-12 < k_{OH} < 3.38E-12 cm^3 $molec^{-1}$ sec^{-1}, assign to **ALK3**.
    d. If 3.38E-12 < k_{OH} < 6.77E-12 cm^3 $molec^{-1}$ sec^{-1}, assign to **ALK4**.
    e. If 6.77E-12 > k_{OH}, assign to **ALK5**.
3. Maintain all other original SAPRC07TC_AE7 assignments.

Figure S1. SOA mass yield vs. log(C*) for 401 VCPy species categorized by their SAPRC07TC_AE7_VCP assignments. White shading indicates the range of VOCs with log(C*) > 6.5, orange shading indicates the range of IVOCs with 2.5 < log(C*) < 6.5, and green shading indicates the range of SVOCs with log(C*) < 2.5. SOA yield increases with decreasing volatility. The method of assigning SOA yields to each species is described in Seltzer et al. (2021) and the SOA yield data is provided in Presto et al. (2010), Tkacik et al. (2012), Cappa & Wilson (2012), McDonald et al. (2018), Ng et al. (2007), Hildebrandt et al. (2009), Janechek et al. (2019), Wu & Johnston (2017), Li & Cocker (2018), and Charan et al. (2020).

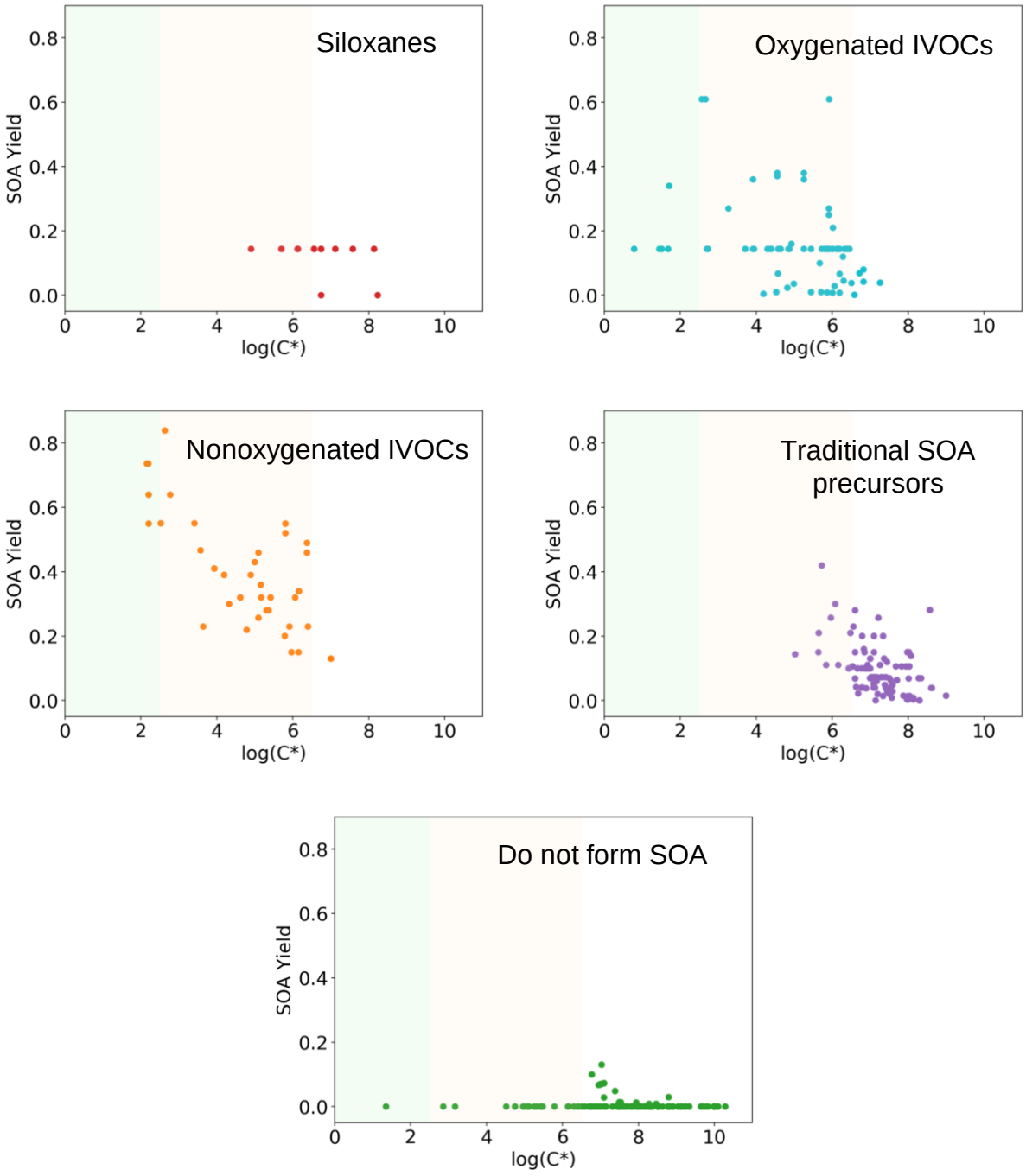

Figure S2. Average hourly concentrations of gas-phase IVOCs (oxygenated + nonoxygenated) predicted by the model for the zero VCP (green) and CMAQv5.3.2 (blue) cases. Horizontal lines depict campaign-average values for hydrocarbon-like IVOCs (6.3 μg m^{-3}) and oxygenated + hydrocarbon-like IVOCs (10.5 μg m^{-3}) from Zhao et al. (2014).

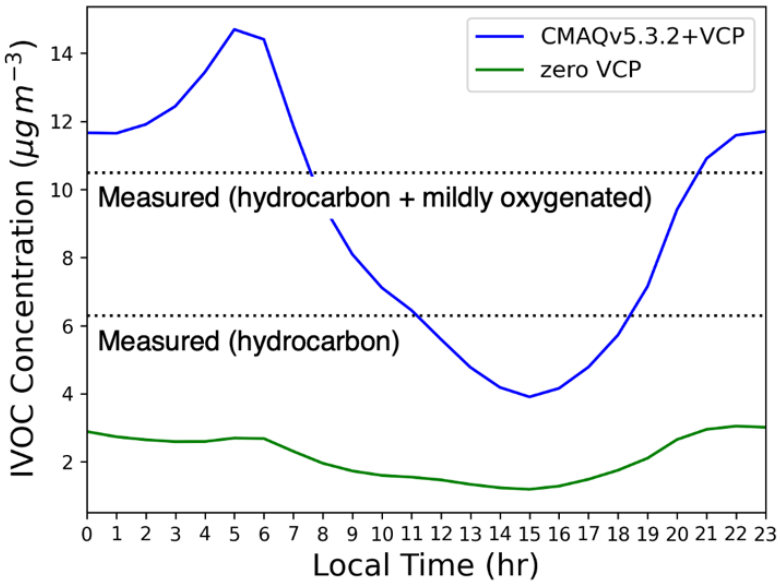

Figure S3. Average hourly concentrations observed and simulated by all three modeling cases May 15-June 15. Box and whiskers show all hourly concentrations observed at the Pasadena CalNex site. a) Background-corrected PM_1 SOA. A constant background value was removed from all observed concentrations according to the method in Hayes et al. (2015). The background value of each simulation was determined by averaging the lower 50% of hourly concentrations from 00:00 LT to 04:00 LT and subtracting that from each curve. b) Formaldehyde (HCHO). Background values were not removed. c) Ozone (O_3). Background values were not removed. d) Carbon monoxide (CO). Background values were not removed. Box and whiskers were removed because they obscured the y-axis scale.

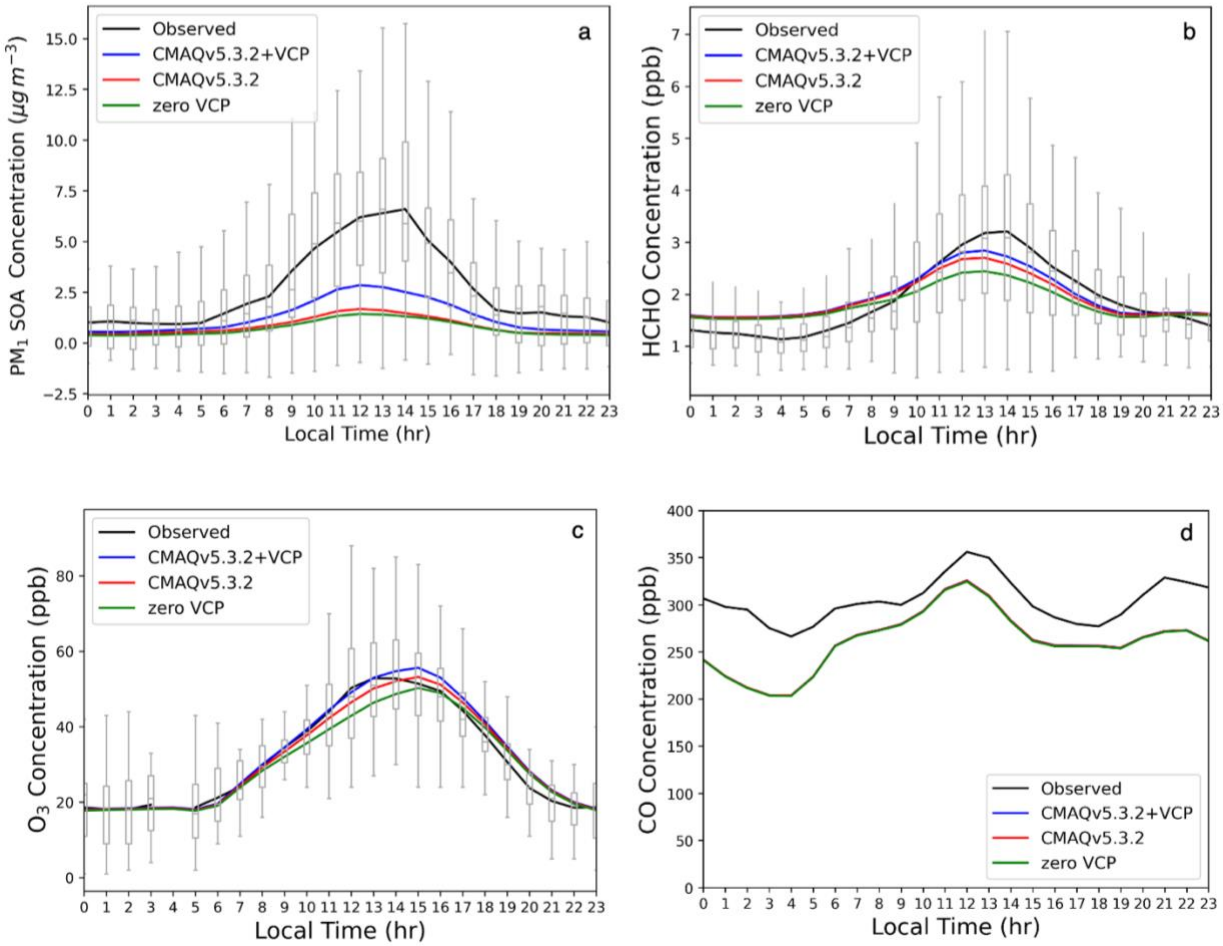

Figure S4. Modeled concentrations predicted by CMAQv5.3.2 case (red) and CMAQv5.3.2+VCP case (blue) vs. observations from the CalNex Pasadena ground site. a) Hourly PM_1 SOA. b) Hourly formaldehyde (HCHO). c) MDA8 O_3. Background values were not removed from any panels.

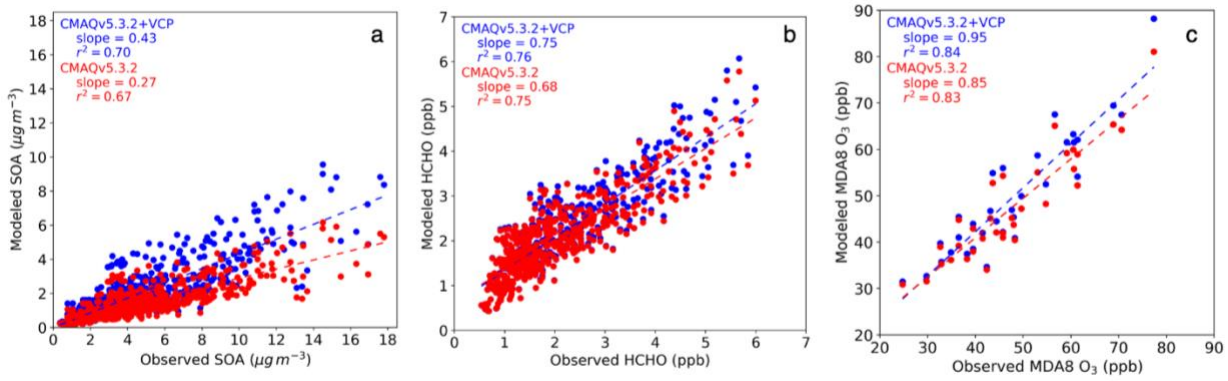

Figure S5. Modeled vs. observed MDA8 O_3 concentration for 178 routine monitoring sites from the AQS monitoring network in California for the zero VCP case (a), CMAQv5.3.2 case (b), and CMAQv5.3.2+VCP case (c).

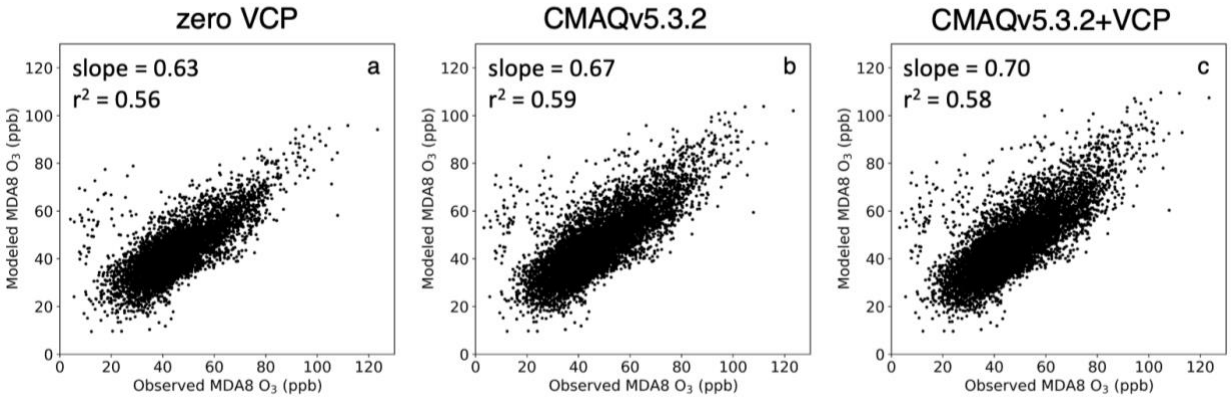

Figure S6. Bias (modeled - observed) of hourly concentrations vs. hourly modeled temperature for the CMAQv5.3.2 case (red) and CMAQv5.3.2+VCP case (blue). a) PM_1 SOA bias (μg m^{-3}). b) PM_1 POA bias (μg m^{-3}). c) Formaldehyde (HCHO) bias (ppb). d) CO bias (ppb).

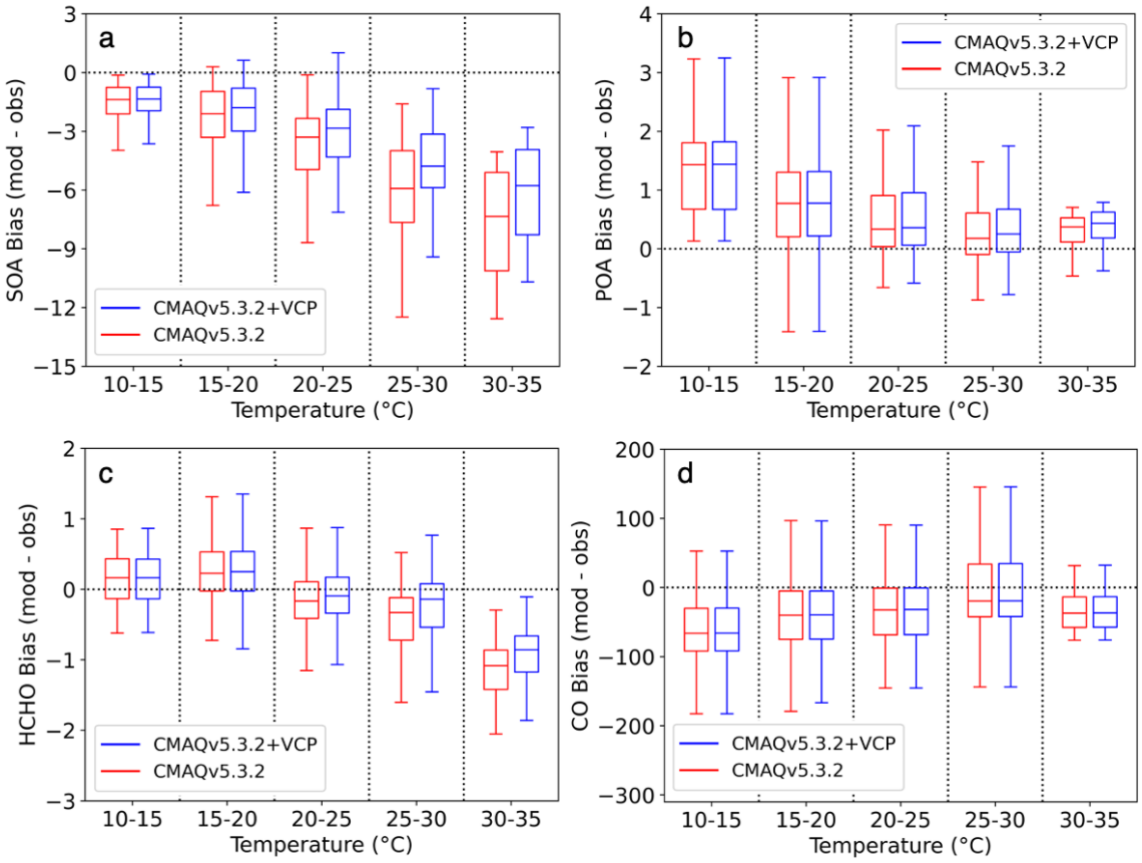

Figure S7. PM_1 SOA (a) and PM_1 POA (b) vs. temperature for zero VCP case (green), CMAQv5.3.2+VCP case (blue), and CalNex observations (black). Background values were not removed from any concentrations.

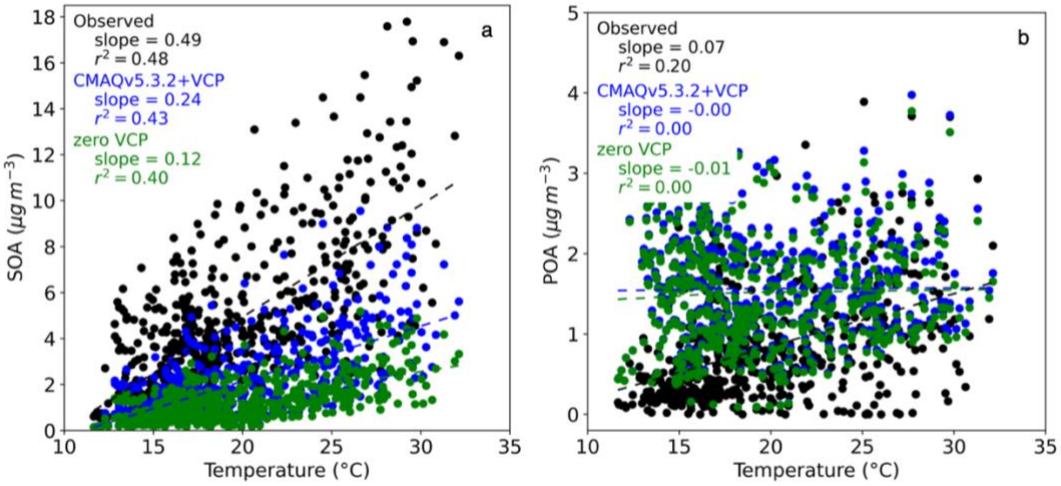

Figure S8. PM_1 SOA vs. PM_1 POA (a), PM_1 SOA vs. CO (b), PM_1 SOA vs. HCHO (c) for zero VCP case (green), CMAQv5.3.2+VCP case (blue), and CalNex observations (black). Background values were not removed from any concentrations.

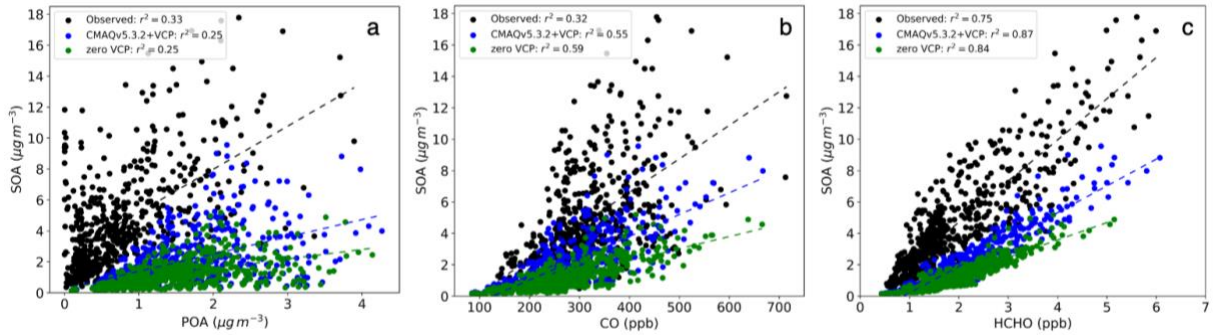

References

Cappa, C. D., & Wilson, K. R. (2012). Multi-generation gas-phase oxidation, equilibrium partitioning, and the formation and evolution of secondary organic aerosol. *Atmospheric Chemistry and Physics*, *12*(20), 9505–9528. https://doi.org/10.5194/acp-12-9505-2012

Carter, W. P. L. (2010). Development of the SAPRC-07 chemical mechanism. *Atmospheric Environment*, *44*(40), 5324–5335. https://doi.org/10.1016/j.atmosenv.2010.01.026

Charan, S. M., Buenconsejo, R. S., & Seinfeld, J. H. (2020). Secondary organic aerosol yields from the oxidation of benzyl alcohol. *Atmospheric Chemistry and Physics*, *20*(21), 13167–13190. https://doi.org/10.5194/acp-20-13167-2020

Hayes, P. L., Carlton, A. G., Baker, K. R., Ahmadov, R., Washenfelder, R. A., Alvarez, S., Rappenglück, B., Gilman, J. B., Kuster, W. C., de Gouw, J. A., Zotter, P., Prévôt, A. S.

H., Szidat, S., Kleindienst, T. E., Offenberg, J. H., Ma, P. K., & Jimenez, J. L. (2015). Modeling the formation and aging of secondary organic aerosols in Los Angeles during CalNex 2010. *Atmospheric Chemistry and Physics*, *15*(10), 5773–5801. https://doi.org/10.5194/acp-15-5773-2015

Hildebrandt, L., Donahue, N. M., & Pandis, S. N. (2009). High formation of secondary organic aerosol from the photo-oxidation of toluene. *Atmospheric Chemistry and Physics*, *9*(9), 2973–2986. https://doi.org/10.5194/acp-9-2973-2009

Janechek, N. J., Marek, R. F., Bryngelson, N., Singh, A., Bullard, R. L., Brune, W. H., & Stanier, C. O. (2019). Physical properties of secondary photochemical aerosol from OH oxidation of a cyclic siloxane. *Atmospheric Chemistry and Physics*, *19*(3), 1649–1664. https://doi.org/10.5194/acp-19-1649-2019

Li, L., & Cocker, D. R. (2018). Molecular structure impacts on secondary organic aerosol formation from glycol ethers. *Atmospheric Environment*, *180*, 206–215. https://doi.org/10.1016/j.atmosenv.2017.12.025

Lu, Q., Murphy, B. N., Qin, M., Adams, P. J., Zhao, Y., Pye, H. O. T., Efstathiou, C., Allen, C., & Robinson, A. L. (2020). Simulation of organic aerosol formation during the CalNex study: Updated mobile emissions and secondary organic aerosol parameterization for intermediate-volatility organic compounds. *Atmospheric Chemistry and Physics*, *20*(7), 4313–4332. https://doi.org/10.5194/acp-20-4313-2020

McDonald, B. C., Gouw, J. A. de, Gilman, J. B., Jathar, S. H., Akherati, A., Cappa, C. D., Jimenez, J. L., Lee-Taylor, J., Hayes, P. L., McKeen, S. A., Cui, Y. Y., Kim, S.-W., Gentner, D. R., Isaacman-VanWertz, G., Goldstein, A. H., Harley, R. A., Frost, G. J., Roberts, J. M., Ryerson, T. B., & Trainer, M. (2018). Volatile chemical products emerging as largest petrochemical source of urban organic emissions. *Science*, *359*(6377), 760–764. https://doi.org/10.1126/science.aaq0524

Ng, N. L., Kroll, J. H., Chan, A. W. H., Chhabra, P. S., Flagan, R. C., & Seinfeld, J. H. (2007). Secondary organic aerosol formation from *m*-xylene, toluene, and benzene. *Atmospheric Chemistry and Physics*, *7*(14), 3909–3922. https://doi.org/10.5194/acp-7-3909-2007

Presto, A. A., Miracolo, M. A., Donahue, N. M., & Robinson, A. L. (2010). Secondary Organic Aerosol Formation from High-NOx Photo-Oxidation of Low Volatility Precursors: N-Alkanes. *Environmental Science & Technology*, *44*(6), 2029–2034. https://doi.org/10.1021/es903712r

Seltzer, K. M., Pennington, E., Rao, V., Murphy, B. N., Strum, M., Isaacs, K. K., & Pye, H. O. T. (2021). Reactive organic carbon emissions from volatile chemical products. *Atmospheric Chemistry and Physics*, *21*(6), 5079–5100. https://doi.org/10.5194/acp-21-5079-2021

Tkacik, D. S., Presto, A. A., Donahue, N. M., & Robinson, A. L. (2012). Secondary Organic Aerosol Formation from Intermediate-Volatility Organic Compounds: Cyclic, Linear, and Branched Alkanes. *Environmental Science & Technology*, *46*(16), 8773–8781. https://doi.org/10.1021/es301112c

US EPA, O. (2019, July 16). *SPECIATE 5.1 and 5.0 Addendum and Final Report* [Other Policies and Guidance]. US EPA. https://www.epa.gov/air-emissions-modeling/speciate-51-and-50-addendum-and-final-report

US EPA Office of Research and Development. (2020). *CMAQ*. Zenodo. https://doi.org/10.5281/zenodo.4081737

Wu, Y., & Johnston, M. V. (2017). Aerosol Formation from OH Oxidation of the Volatile Cyclic Methyl Siloxane (cVMS) Decamethylcyclopentasiloxane. *Environmental Science & Technology*, *51*(8), 4445–4451. https://doi.org/10.1021/acs.est.7b00655

Zhao, Y., Hennigan, C. J., May, A. A., Tkacik, D. S., de Gouw, J. A., Gilman, J. B., Kuster, W. C., Borbon, A., & Robinson, A. L. (2014). Intermediate-Volatility Organic Compounds: A Large Source of Secondary Organic Aerosol. *Environmental Science & Technology*, *48*(23), 13743–13750. https://doi.org/10.1021/es5035188